A Generalized Geo-Electro-Mechanical Model for Triboelectric NanoGenerators

Mohammed Shehata[1], Eslam A. Aly[1], Mostafa B. Alabd[1] and Hassan Mostafa[1,2]
[1]Electronics and Electrical communications Engineering Department, Faculty of Engineering, Cairo University, Giza 12613, Egypt.
[2]Nanotechnology Department at Zewail City for Science and Technology, Cairo, Egypt.
Email: hmostafa@uwaterloo.ca

***Abstract*—Different energy harvesting techniques have gathered the attention of many, due to the huge potential they hold in future technologies. Among these newly emerging techniques are the triboelectric nanogenerators (TENGs). TENGs hold great potential, and prove very promising as reliable power sources for small, mobile electronic devices, and mobile sensor networks.**
In this paper, the attached-electrode contact-mode (AE-CM) TENG is investigated and analytically modeled. The modeling of any TENG can be broken down in three parts; the external mechanical excitation and the resulting geometrical effects, the equivalent electrical model due to the geometrical changes in its structure, and the integration of the equivalent electrical model with external loads.
This approach is adopted in this work, and it greatly matches the results obtained experimentally and by simulation as will be discussed later in the paper.

***Index Terms*—Triboelectric nanogenerators, TENG, Energy harvesters, renewable energy, attached-electrode, AE-CM.**

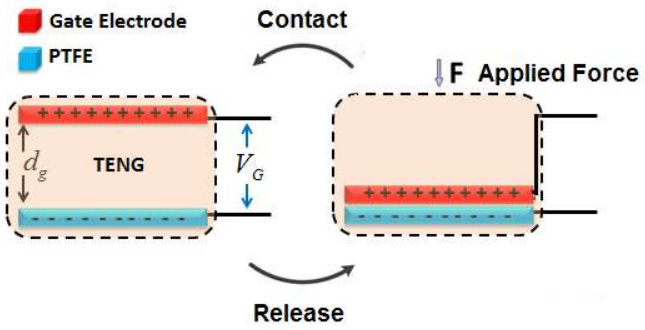

Fig. 1. The working mechanism of the attached-electrode contant-mode TENG

I. INTRODUCTION

With the rapid growth of portable electronic devices and sensor networks, providing sustainable, mobile, and stable sources of energy becomes mandatory. Although conventional chemical energy-based batteries are usually used in similar applications, their use is not desired for various reasons [1]. Therefore, harvesting the ambient energy to provide sustainable, clean and reliable power sources in similar applications is the motivation for this work.

Recently, energy harvesting technologies have gained a lot of attention, especially in the last decade. They are being developed and optimized on a very fast pace [2], implementing different techniques to harvest different kinds of ambient energy [3]. Triboelectric nanogenerators (TENGs) are one of the newly emerging and promising energy harvesting technologies. Mainly due to its unique merits, such as high conversion efficiency, low weight and ease of fabrication [4].

Throughout the literature, great efforts have been dedicated to characterizing TENGs, either experimentally or by simulation [4]. However, to the best of the authors knowledge, no analytical models have yet been reported to characterize TENGs and their operation.

This work provides a systematic, multi-physics-based modeling approach for TENGs, it provides a reliable framework to model different modes of TENGs, which proves very convenient for the simulation and analysis of TENGs as a black-box. The proposed approach relies on breaking down the TENG system into three cascaded sub-systems, each of which is accurately modeled and characterized. This model shows an excellent match with the previously reported experimental and simulation results as will be discussed [4].

The paper is organized as follows; in section II, the principles and different modes of operation of TENGs are overviewed. in section III, TENG, as a geo-electro-mechanical system, is modeled and characterized with aided simulation results.

II. PRINCIPLES OF OPERATION

TENGs operation is fundamentally a conjugation of the contact electrification and electrostatic induction [5]. The contact-separation motion between the two triboelectric materials causes charged particles to be released as bonds are broken between the molecules of the two materials. it causes the facing surfaces of the two materials to be oppositely charged which results in a potential difference [4].

A. Fundamental modes of TENGs

As stated in previous work [4], TENGs are classified into four fundamental modes, this classification is based on the electrostatic induction process for each mode, and its working mechanism. The four basic modes of TENGs are; the attached-electrode contact-mode (AE-CM) TENG, attached-electrode sliding-mode TENG, single electrode TENG, and

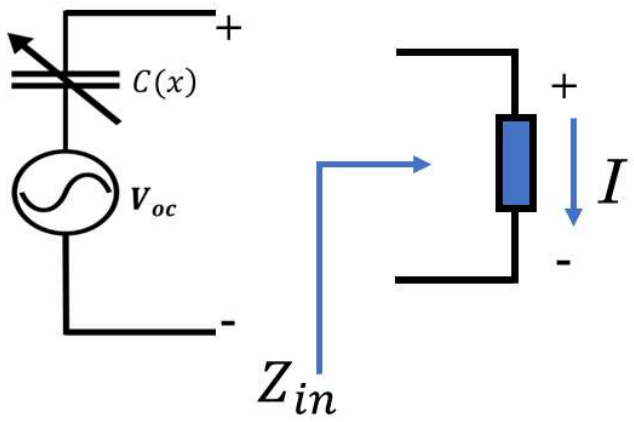

Fig. 2. First-order lumped-parameter equivalent circuit model of TENG

Freestanding-triboelectric-layer based TENG. The attached-electrode contact-mode TENGs, as shown in Fig. 1, are the main focus of this work.

The working mechanism of the AE-CM TENGs is as follows, initially, a mechanical-mechanical contact interaction takes place between an externally applied force and one of the two plates, resulting in a motion of this plate towards or outwards the stationary second plate. When the two triboelectric materials are brought into contact, contact electrification then takes place and the two triboelectric materials act as a charged parallel-plate capacitor, which has a time-dependent capacitance. This information comes in handy when modeling the geo-mechanical stage of the AE-CM TENG in section III.

B. The governing V-Q-x relationship and first-order lumped-parameter circuit model

As previously derived in [4], the $V-Q-x$ relationship (1) is the governing equation for the AE-CM TENG as a two-terminal electrical device, specifically stating the inherent capacitive nature of TENGs and its resemblance to the parallel plate capacitor. Thus, the electrical potential difference between the two electrodes is a result of both the electric field caused by the charges on the facing surfaces of the parallel plates and the polarized triboelectric charges and their contribution to the $V_{OC}(x)$. As a result, electrical charges are driven through the two electrodes into an externally connected circuit.

$$V = -\frac{1}{C(x)}Q + V_{oc}(x) \tag{1}$$

where, x is the distance between the two plates. As shown in the $V-Q-x$ relationship of TENGs, the lumped-parameter first-order equivalent circuit model can be easily derived. The two terms on the right-hand side of (1) can be represented by a series-connected voltage source $V_{OC}(x)$ and a variable capacitor $C_T(x)$, as illustrated in Fig. 2. This equivalent circuit model is further discussed in section III as it represents the second stage of the AE-CM TENGs.

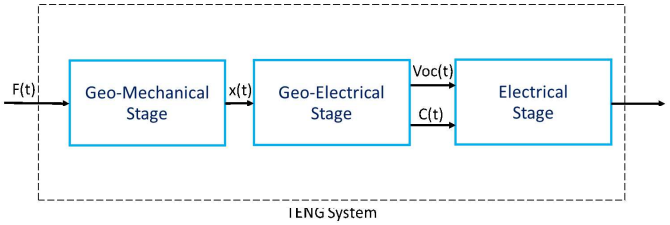

Fig. 3. The Geo-Electro-Mechanical model of the AE-CM TENGs

III. Geo-electro-mechanical model

Energy harvesting using TENGs is a complicated process that involves multiple physical phenomena. On the microscopic level, the physical phenomena taking place between the triboelectric materials are still under investigation by quantum mechanics practitioners and material engineers [6]. However, from a macroscopic viewpoint, a TENG is simply an electro-mechanical energy conversion system. The energy acquired by the mechanical system during the contact phase is stored and converted to electrical energy at the output terminals of the system.

As aforementioned, the AE-CM TENGs are modeled in this work as the cascade of three sub-systems, as shown in Fig. 3, the geo-mechanical stage which converts the external mechanical excitation to spatial displacement, the geo-electrical stage which converts the spatial displacement to an electrical equivalent, and finally the electrical stage which interfaces the electrical model of TENG with different types of loads.

It's worth mentioning that the main difference between the TENG modes is in the geo-mechanical stage, as they have different geometrical structures and would require unique modeling of this stage for each mode or structure, while the other two stages may remain unchanged from the AE-CM TENG discussed later. Thus, the geo-mechanical stage of the AE-CM TENGs is the main focus of this work. In this section, the geo-electro-mechanical model of TENGs, illustrated in Fig. 3, is analytically derived and proved to be fully compliant with simulation and experimental results.

A. Geo-mechanical model

Simple harmonic motion (SHM) is one of the simplest forms of periodic motions to study. Furthermore, it is a common kind of interaction in our daily life. Thus, analyzing the AE-CM TENG Geo-Mechanical sub-system under SHM input excitation. In this sub-section, the first stage of the AE-CM TENG is modeled as a damped mass-spring mechanical system, as shown in Fig. 4, under harmonic force. Thus, the equation of motion is in the form

$$m\ddot{x} + b\dot{x} + kx = F_{\circ}\cos(\omega t) \tag{2}$$

where m is the mass of the moving plate, b is the viscosity coefficient between the two tribomaterials, k is the spring constant, and F_o is the magnitude of the driving force.

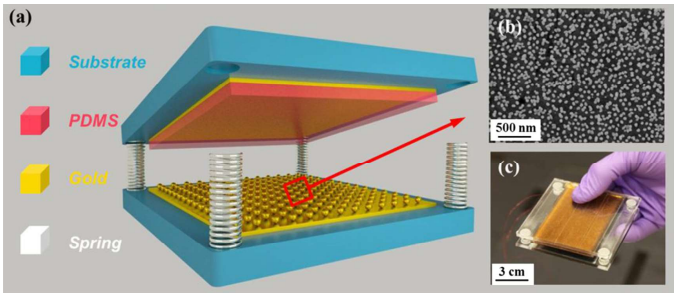

Fig. 4. A schematic of the mechanical model of the contact-mode TENGs [9]

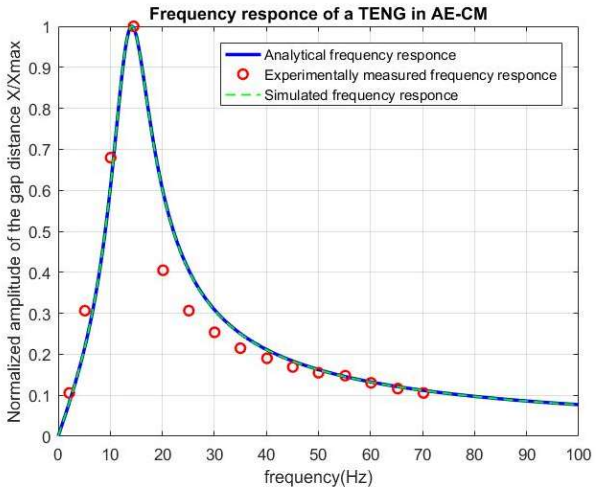

Fig. 5. The frequency response of the geo-mechanical stage of TENGs measured analytically, experimentally [4] and using Cadence CAD simulation tool

Its a common practice to apply the Laplace transformation techniques on linear systems to achieve a more convenient characterization in the S-domain. Therefore, by doing a simple S-domain transformation on the 2^{nd}-order differential equation (2) we can obtain the transfer function of the Geo-Mechanical stage of AE-CM TENGs (3)

$$H(S) = \frac{K.s}{s^2 + \frac{b}{m}s + \frac{k}{m}} \tag{3}$$

where $K = 1/m$. Although the S-domain transfer function of this mass-spring system does not include a differential S-domain operator when applied on (2), the existence of this operator is imposed by the contact adhesion force observed between the thin gold film and the PDMS layer[7]. This transfer function successfully agrees with the results obtained empirically [8] as illustrated in Fig. 5.

Furthermore, it was also realized that (3) matches the transfer function of an active bandpass filter [10], shown in Fig. 6. Therefore, by utilizing the parameters of this active bandpass filter circuit, it can completely match the transfer function of the geo-mechanical stage of the AE-CM

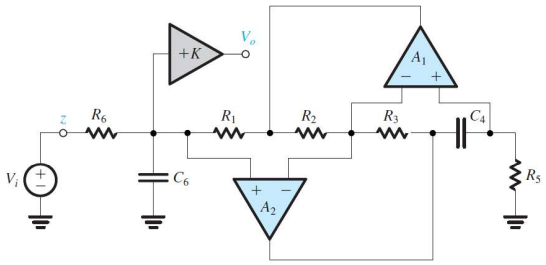

Fig. 6. The active bandpass filter circuit [10]

of TENGs. This realization makes simulating and optimizing the geo-mechanical stage of the AE-CM TENGs very time-efficient while maintaining the accuracy of the results.
Simulation results are obtained, as shown in Fig. 5, these results are based on the electrical-circuits CAD tool Cadence. Fig. 5 clearly illustrates the agreement of the simulation results, the analytical results, and the empirically obtained data [4] representing the first stage of the AE-CM TENGs.

B. Geo-electrical model

Derived from the $V-Q-x$ relation (1) [4], the open circuit voltage and the inherent capacitance of AE-CM TENGs are shown to be dependent on the gap distance $x(t)$ (4) (5). These equations are based on the implicit assumption of the great resemblance of the AE-CM TENGs to the infinite parallel plate capacitor. However, simulation results obtained by the finite element method (FEM) [4] show that this assumption is not completely accurate, Fig. $7(a)$, (b) shows the exact $V_{OC}(x)$ and $C_T(x)$ relationships.

$$V_{OC} = \frac{\sigma x(t)}{\varepsilon_o} \tag{4}$$

$$C_T = \frac{\varepsilon_o A}{d_o + x(t)} \tag{5}$$

where, A is the area size, and d_o is the effective dielectric thickness which is defined as follows

$$d_o = \sum_{i=1}^{n} \frac{d_i}{\varepsilon_{ri}} \tag{6}$$

where, n is the number of dielectrics.

As Fig. $7(a)$ suggests, the linear relation (4) does not match the simulation results obtained by the FEM [4]. This work suggests a more accurate linear representation for the $V_{OC}-x$ relationship, simply by curve-fitting the simulation results in Fig. $7(a)$ and then deriving its tangent line at $x = 0.04cm$, as illustrated by the dashed line. Thus, we conclude a more accurate representation of the $V_{OC} - x$ linear relation.
The $V_{OC} - x$ relationship is derived more accurately by solving Poissons equation for the spatial distribution of the electrostatic potential using the FEM or any suitable numerical method [11]

$$\nabla^2\psi(x(t), y, z) = -\frac{\sigma_e}{\varepsilon} \tag{7}$$

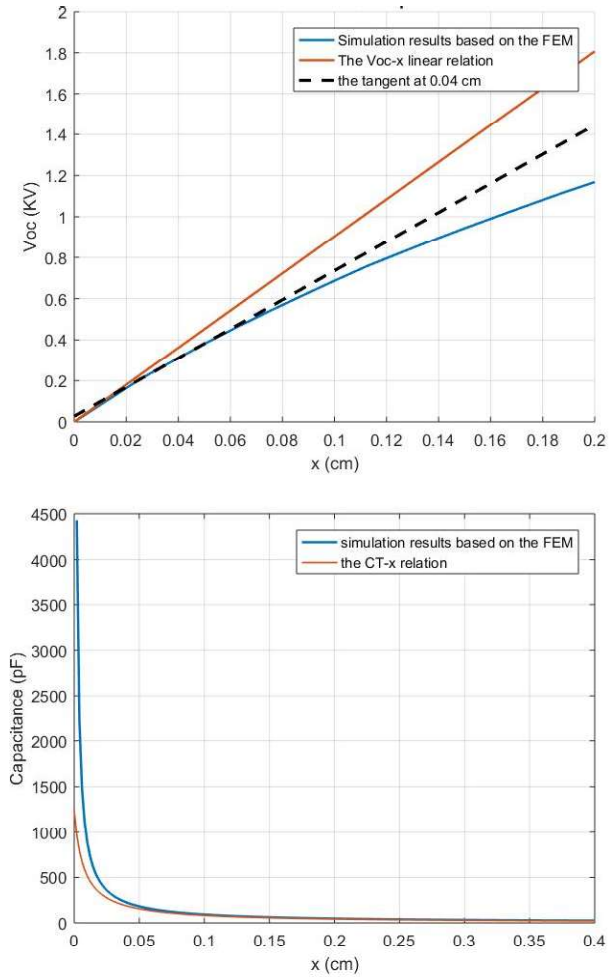

Fig. 7. The intrinsic output characteristics of AE-CM TENGs. $(a)$the open circuit voltage, $(b)$the capacitance between the two electrodes

Furthermore, The $C_T - x(t)$ relationship shows great agreement with the simulation results. However, a more accurate analytical form is derived in this work [12].

C. Electrical model

As the final stage of the geo-electro-mechanical model of TENGs, this stage connects the TENG as a two-terminal Thevenin equivalent circuit to external load, as shown in Fig. 2. This stage is particularly useful when interfacing TENGs with external electronic devices in the context of a bigger system. The performance of such electrical systems has been extensively studied either theoretically, experimentally, or by simulation.

Characterizing this stage of the TENG is very simple using the circuit theory, and depending on the present load, one can tune and optimize TENGs parameters to achieve optimum performance [4].

IV. Conclusion

As demonstrated in this paper, the AE-CM TENGs are analytically characterized as a geo-electro-mechanical system, which consists of three cascaded sub-systems as previously discussed. The main focus of this work is modeling the geo-mechanical stage of the AE-CM TENGs as it differs for every mode of TENGs while the last two stages may not. Also, the last two stages are previously characterized and modeled in literature, and it was re-investigated in this work. This model shows great matching with the previously obtained simulation and experimental results. This model provides a systematic framework of modeling different modes of TENGs, which proves as a reliable design guideline for the development and utilization of TENGs as the power source for different types of systems.

V. Acknowledgment

This work was partially funded by ONE Lab at Zewail City of Science and Technology and Cairo University, NTRA, ITIDA, ASRT, Mentor Graphics, NSERC.

References

[1] A. Bernardes, D. Espinosa, and J. Tenrio, "Recycling of batteries: a review of current processes and technologies," *Journal of Power Sources*, vol. 130, no. 1, pp. 291 – 298, 2004.

[2] G. K. Ottman, H. F. Hofmann, and G. A. Lesieutre, "Optimized piezoelectric energy harvesting circuit using step-down converter in discontinuous conduction mode," *IEEE Transactions on Power Electronics*, vol. 18, pp. 696–703, March 2003.

[3] S. Priya and D. J. Inman, *Energy harvesting technologies*, vol. 3. 2010.

[4] S. Niu and Z. L. Wang, "Theoretical systems of triboelectric nanogenerators," *Nano Energy*, vol. 14, pp. 161 – 192, 2015. Special issue on the 2nd International Conference on Nanogenerators and Piezotronics (NGPT 2014).

[5] F.-R. Fan, Z.-Q. Tian, and Z. L. Wang, "Flexible triboelectric generator," *Nano Energy*, vol. 1, no. 2, pp. 328 – 334, 2012.

[6] N. Cui, L. Gu, Y. Lei, J. Liu, Y. Qin, X. Ma, Y. Hao, and Z. L. Wang, "Dynamic behavior of the triboelectric charges and structural optimization of the friction layer for a triboelectric nanogenerator," *ACS Nano*, vol. 10, no. 6, pp. 6131–6138, 2016. PMID: 27129019.

[7] F. Leite, C. C Bueno, A. Rz, E. Ziemath, and O. Oliveira 2012.

[8] J. Chen, G. Zhu, W. Yang, Q. Jing, P. Bai, Y. Yang, T.-C. Hou, and Z. L. Wang, "Harmonic-resonator-based triboelectric nanogenerator as a sustainable power source and a self-powered active vibration sensor," *Advanced Materials*, vol. 25, no. 42, pp. 6094–6099, 2013.

[9] G. Zhu, B. Peng, J. Chen, Q. Jing, and Z. L. Wang, "Triboelectric nanogenerators as a new energy technology: From fundamentals, devices, to applications," *Nano Energy*, vol. 14, pp. 126 – 138, 2015. Special issue on the 2nd International Conference on Nanogenerators and Piezotronics (NGPT 2014).

[10] A. S. Sedra and K. C. Smith, *Microelectronic Circuits*. Oxford University Press, fifth ed., 2004.

[11] C. Pennisi, E. Greenbaum, and K. Yoshida, "Spatial distribution of the electric potential from photosystem i reaction centers in lipid vesicles," *IEEE transactions on nanobioscience*, vol. 7, pp. 164–71, 07 2008.

[12] M. Hosseini, G. Zhu, and Y.-A. Peter, "A new formulation of fringing capacitance and its application to the control of parallel-plate electrostatic micro actuators," *Analog Integrated Circuits and Signal Processing*, vol. 53, pp. 119–128, 12 2007.

[13] M. S. Y. I. Zaky, Ahmed and H. Mostafa, "Characterization and model validation of triboelectric nanogenerators using verilog-a.," *In 2017 IEEE 60th International Midwest Symposium on Circuits and Systems (MWSCAS), pp. 1536-1539. IEEE, 2017.*

[14] A. M. F. A. S. T. A. A. Maximous, George S. and H. Mostafa, "A new cad tool for energy optimization of diagonal motion mode of attached electrode triboelectric nanogenerators.," *In 2018 16th IEEE International New Circuits and Systems Conference (NEWCAS), pp. 331-334. IEEE, 2018.*

[15] A. A. P. I. B. M. Zaky, Ahmed and H. Mostafa, "In-out cylindrical triboelectric nanogenerators based energy harvester.," *In 2018 IEEE 61st International Midwest Symposium on Circuits and Systems (MWSCAS), pp. 1118-1121. IEEE, 2018.*